Abdominal Radiology (2019) 44:2511–2527
https://doi.org/10.1007/s00261-019-01988-3

REVIEW

The inferior vena cava: a pictorial review of embryology, anatomy, pathology, and interventions

David S. Shin[1] · Claire K. Sandstrom[1] · Christopher R. Ingraham[1] · Eric J. Monroe[1,2] · Guy E. Johnson[1]

Published online: 1 April 2019
© Springer Science+Business Media, LLC, part of Springer Nature 2019

Abstract
The inferior vena cava (IVC) is the largest venous conduit below the diaphragm. Although this structure is often overlooked both clinically and radiographically, it can be involved in many different pathologic processes. A thorough understanding of the IVC will assist the radiologist in recognizing anatomic variants, identifying abnormalities, and providing accurate differential diagnoses. In this comprehensive pictorial review of the IVC, we depict embryology behind anatomic variants, present a wide range of pathology with a focus on diagnostic imaging, and describe relevant endovascular interventions.

Keywords Inferior vena cava · Embryology · Anatomic variants

Introduction

The IVC is the primary conduit for venous return from the lower extremities, pelvis, kidneys, and abdominal viscera. It can be an easy structure to overlook on imaging unless there is a gross abnormality. Disease processes primarily or secondarily involving the IVC, such as tumor or thrombosis, often present in late stages, and can pose a diagnostic challenge clinically. The radiologist can play a critical role in timely diagnosis of pathology involving the IVC. A thorough knowledge of anatomy, anatomic variants, and the multitude of diseases that affect the IVC is central to the diagnosis of IVC abnormalities.

This imaging review begins with a discussion on the basic embryology and anatomic variants of the IVC, followed by a case-based illustration of common IVC pathology, including tumors, thrombosis, and trauma. Fundamental interventional techniques involving the IVC will then be reviewed.

✉ David S. Shin
dsshin@uw.edu

[1] Department of Radiology, University of Washington, 1959 NE Pacific St, Box 357115, Seattle, WA 98195, USA

[2] Department of Radiology, Seattle Children's Hospital, Seattle, WA, USA

Basic embryology

The intricate ontogeny of the IVC begins with three paired venous networks in the early weeks of embryonic life [1] (Fig. 1). The posterior cardinal, subcardinal, and supracardinal veins develop sequentially. Ultimately, the orthotopic (right-sided) IVC is a composite structure formed when some parts of these venous networks anastomose and others regress. The suprarenal IVC forms from the right subcardinal vein. The infrarenal IVC originates from the right supracardinal vein. The renal segment of the IVC forms after the right and left subcardinal venous anastomoses coalesce. Anomalous IVC anatomy may result from abnormal persistence or regression of these fetal venous structures.

Anatomic variants

The most common variants in IVC anatomy are a duplicated IVC and a left IVC. A duplicated IVC results when both the right and left supracardinal veins persist (Fig. 2). This variant is seen in 0.2–3% of the population. Generally, when a duplicated IVC is present, the left moiety drains into left renal vein, which in turn usually joins with the right IVC, leading to the normal suprarenal anatomy. Iliac venous inflows into the duplicated system may be isolated to each respective side or may join at the inferior origin of the duplicated IVC.

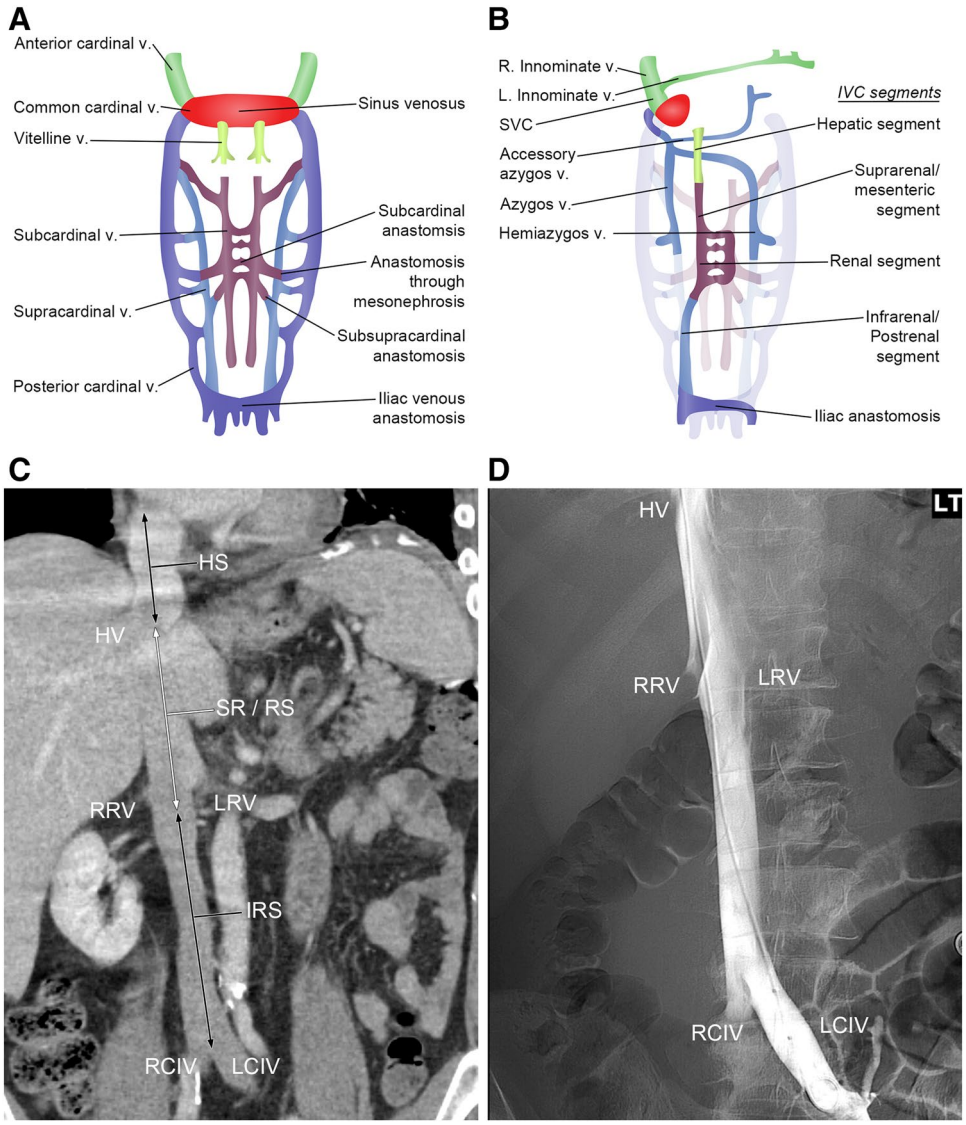

Fig. 1 Normal IVC. **a** At 6–7 weeks of fetal development, three paired venous structures are identified—the posterior cardinal veins, subcardinal veins, and supracardinal veins—with anastomoses connecting them. *Graphics created by CKS*. **b** Normal right-sided IVC is formed by the persistence of the suprarenal segment of the right subcardinal vein (suprarenal IVC), fused renal segments of the bilateral subcardinal veins (renal segment of the IVC), the infrarenal portion of the right supracardinal vein (infrarenal IVC), and the iliac anastomosis of the posterior cardinal veins (common iliac vein confluence). The hepatic and supradiaphragmatic segments of the IVC arise from the vitelline vein. The superior portions of the bilateral supracardinal veins give rise to the azygos–hemiazygos venous system. *Graphics created by CKS*. **c** Coronal contrast-enhanced CT image from a 54-year-old man shows normal IVC anatomy. Double arrows indicate the IVC segments derived from different fetal structures: HS, hepatic segment; SR/RS, suprarenal/renal segment; IRS, infrarenal segment. Important venous inflows include right and left common iliac veins (RCIV and LCIV), right and left renal veins (RRV and LRV), and hepatic veins (HV). **d** Unsubtracted inferior vena cavogram from the same patient shows the normal right-sided IVC. Contrast was injected into the left common iliac vein (LCIV), while expected unopacified inflow artifacts are seen from the right common iliac vein (RCIV), right renal vein (RRV), left renal vein (LRV), and hepatic veins (HV)

If there is abnormal persistence of the left supracardinal vein with regression of the right supracardinal vein, the result is a left IVC (Fig. 3). This variant is rarer than the duplicated IVC and has a prevalence of 0.2–0.5%. As with duplicated IVC, the left IVC usually terminates at the level of the left renal vein, which joins the orthotopic suprarenal IVC.

A circumcaval (also termed retrocaval) ureter, despite the terminology, represents a rare anatomic variant of the IVC (Fig. 4). It occurs when there is persistence of the right posterior cardinal vein with abnormal regression of the right supracardinal vein. Although the IVC is orthotopic, the right ureter follows a spiraling course around the cava. The proximal ureter courses inferomedially and crosses the IVC posteriorly, then

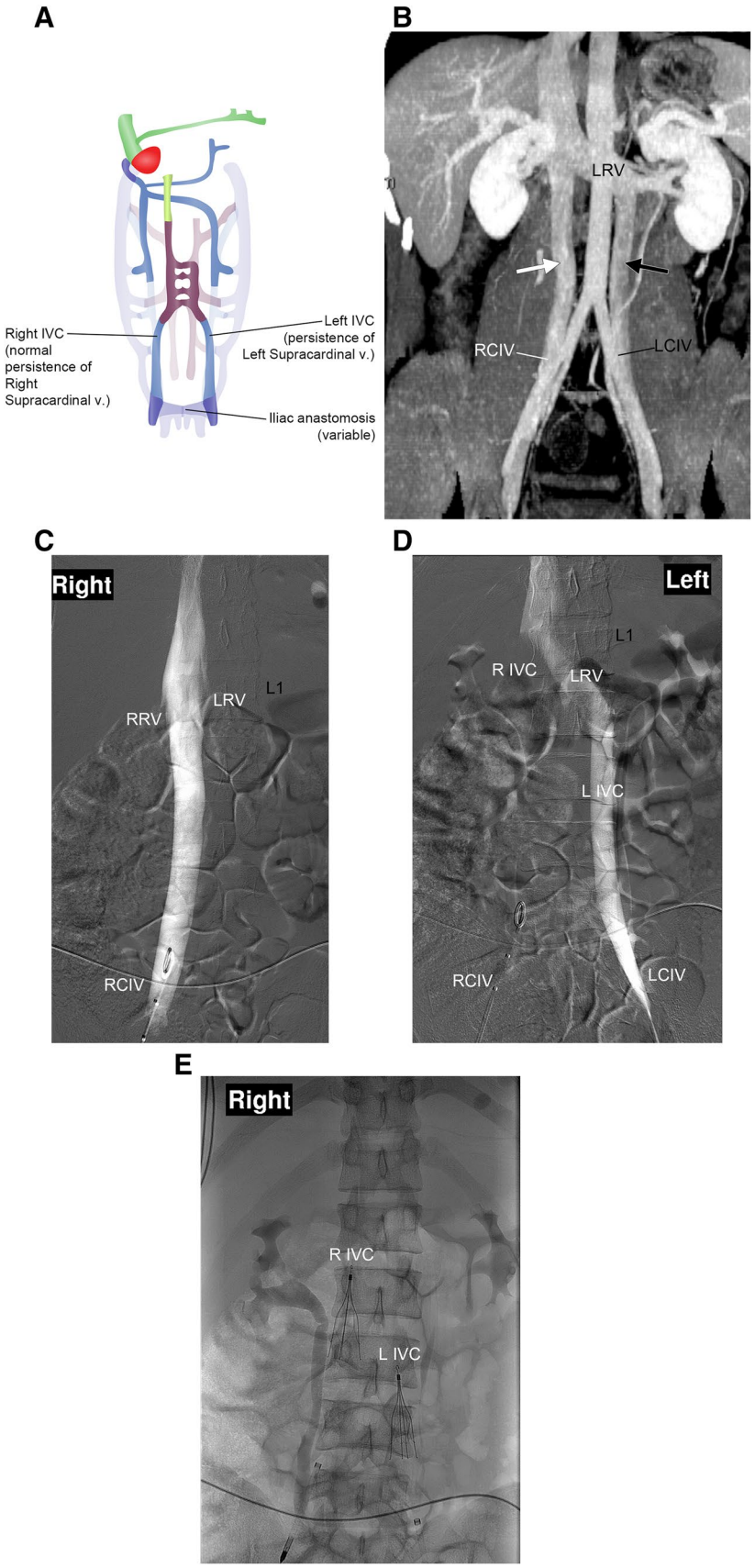

Fig. 2 Duplicated IVC. **a** Persistence of the infrarenal segment of the left supracardinal vein and the iliac portion of the left posterior cardinal vein creates IVC duplication. There is variable persistence or regression of the iliac anastomosis between the posterior cardinal veins, such that there may or may not be communication between the bilateral common iliac veins. *Graphics created by CKS*. **b** Coronal maximum-intensity projection CT image from a 38-year-old man shows a left-sided IVC (black arrow), which joins the left renal vein (LRV), which in turn joins the right-sided IVC (white arrow). In this patient, the right common iliac vein (RCIV) and left common iliac vein (LCIV) remain separate. **c**–**e** A similar pattern of duplicated IVC is shown on digital subtraction venogram images in a 19-year-old man prior to IVC filter placement. **c** Initially, right femoral access with selective injection of the right common iliac vein (RCIV) revealed normal inflow artifacts from the right and left renal veins (RRV and LRV) at about the L1 level. However, no inflow from the left common iliac vein was seen. **d** Subsequent injection at the left common iliac vein (LCIV) confirms a left-sided IVC (L IVC) joining the left renal vein (LRV), which in turn joins the right-sided IVC (R IVC). **e** Two IVC filters were placed, one in each infrarenal IVC moiety

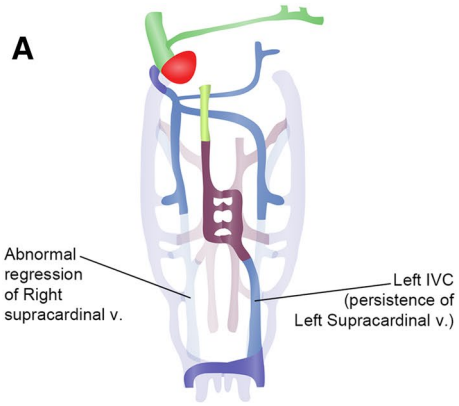

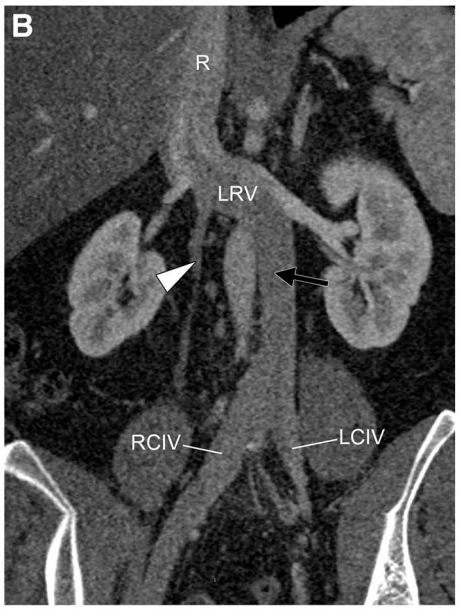

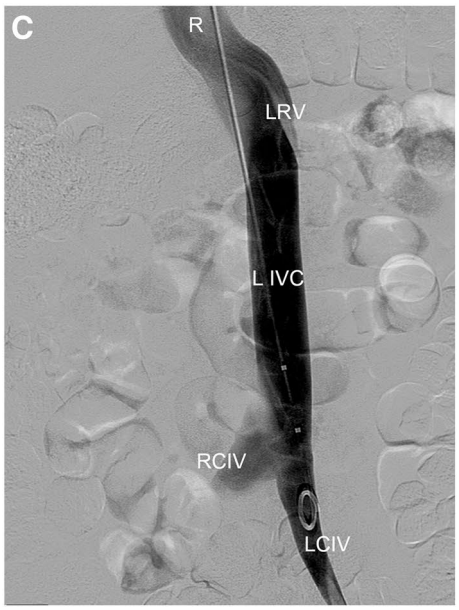

Fig. 3 Single left-sided IVC. **a** Persistence of the infrarenal segment of the left supracardinal vein and abnormal regression of the right supracardinal vein create a single left-sided IVC. The right common iliac vein drains into the left-sided IVC via the iliac anastomosis. *Graphics created by CKS*. **b** Coronal curved reformat CT image from a 47-year-old woman shows the right common iliac vein (RCIV) crossing midline to join the left common iliac vein (LCIV) and forming a left-sided IVC (black arrow). The infrarenal IVC joins the left renal vein (LRV), crosses midline, and becomes the orthotopic right-sided suprarenal IVC (R). The vertically oriented vein to the right of midline is the right gonadal vein (white arrowhead), not to be confused with a remnant right-sided IVC. **c** A similar pattern of left-sided IVC is shown on digital subtraction venogram in a 27-year-old woman. Injection into the left common iliac vein (LCIV) opacifies the left-sided IVC (L IVC), with inflow artifacts from the right common iliac vein (RCIV) and left renal vein (LRV). The suprarenal IVC is on the right (R)

wraps around and descends anterior to the cava. This can result in urinary reflux or obstruction, which, in severe cases, may require surgical reimplantation of the ureter.

Anomalies of the suprarenal IVC are less common. Azygos continuation of the IVC describes a rare variant in which the right subcardinal vein fails to join the vitelline vein to form the intrahepatic IVC [2] (Fig. 5). The azygos vein then assumes the role of predominant venous return from below the diaphragm. The IVC continues superiorly as the right-sided azygos vein, which passes posterior to the diaphragm to the right of the aorta and joins with the SVC in the mediastinum. In this case, the hepatic veins, which derive separately from the embryonic vitelline vein, drain directly into the right atrium. This anomaly is associated with heterotaxy syndrome, especially polysplenia. Rarely, an anomalous left IVC may continue as the hemiazygos vein, passing behind the left diaphragmatic crus to the left of the aorta and ultimately draining into the SVC [3] (Fig. 6).

The diameter of the IVC can vary considerably. However, early angiographic studies have demonstrated the mean IVC diameter to range between 20 and 23 mm in most patients [4, 5]. Megacava is defined as an infrarenal IVC that measures greater than 28 mm in diameter (Fig. 7). This size threshold was originally reported for its increased risk of device failure and migration with IVC filters [5]. Megacava has a prevalence of about 1–2% of patients undergoing imaging of the IVC and can be seen more frequently in patients with right heart failure. Knowledge of this variation in IVC diameter is essential for the correct sizing of devices for interventional procedures (e.g., stents or filters). No retrievable IVC filter has been approved for use in megacava.

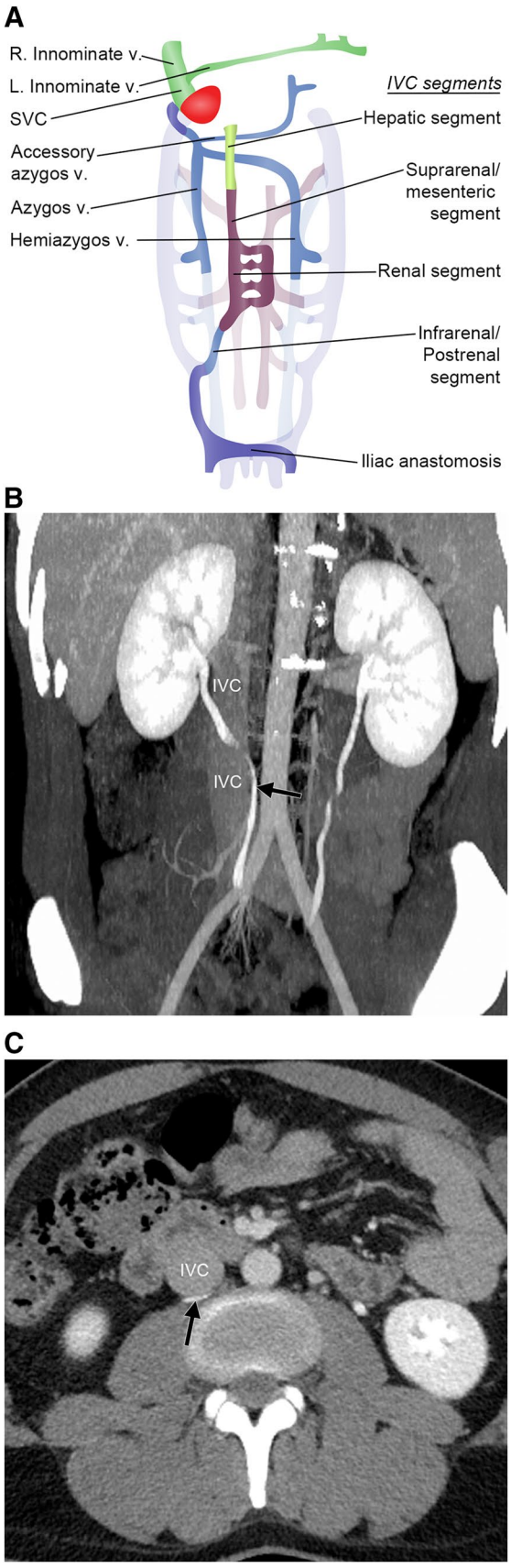

Fig. 4 Circumcaval right ureter. **a** Abnormal regression of the right supracardinal vein and persistence of the caudal portion of the right posterior cardinal vein result in this anatomic variant. *Graphics created by CKS*. **b** Coronal maximum-intensity projection CT image from a 37-year-old man demonstrates the contrast-opacified right ureter (black arrow) wrapping around the orthotopic IVC. **c** On axial CT image, the proximal right ureter (black arrow) passes posterior to the IVC

Diseases involving the IVC

Neoplasm

Malignant involvement of the IVC can be primary or secondary, often characterized by expansile and enhancing intraluminal mass (i.e., tumor thrombus) in either case [6]. Intravascular tumor should be differentiated from bland thrombus especially in hypercoagulable patients with underlying malignancy [7], as the latter may respond well to anticoagulation, while the former will not. When symptomatic, abdominal pain and lower extremity edema are most likely to be reported [8].

Secondary IVC malignancy usually results from intravascular extension of tumor from a solid organ via its venous outflow to the IVC. This can be seen with primary tumors of the liver, kidney, and adrenal gland. In such cases, the tumor thrombus is contiguous with the primary tumor within the organ of origin (Fig. 8).

Renal tumors

Renal cell carcinoma (RCC) is the most common malignancy to involve the IVC [7], with caval extension seen in 4–10% (Figs. 8, 9). Any venous tumor thrombus is considered Robson Stage IIIa, while in the Internal Union Against Cancer tumor-node-metastasis (TNM) classification, renal vein only, infradiaphragmatic IVC, and supradiaphragmatic IVC involvements correspond to T3b, T3c, and T4b, respectively [9] (Fig. 9c). CT has been shown to have negative and positive predictive values for venous extension of 97% and 92%, respectively, with the corticomedullary phase of enhancement being most useful [9].

The standard of care for RCC with vascular invasion is cytoreductive nephrectomy and tumor thrombectomy without or with IVC resection and reconstruction [10]. The need for IVC resection arises in a minority of patients (6–8%) and often cannot be predicted preoperatively. Baseline CT features associated with an increased likelihood of IVC resection include right-sided tumor, IVC anteroposterior diameter > 24 mm at the right renal vein ostium, or complete IVC occlusion at the right renal vein ostium [10]. The Mayo system describes the level of RCC tumor thrombus, and associated surgical treatment, for renal vein and IVC involvement [11] (Fig. 9c). Complete removal of RCC with

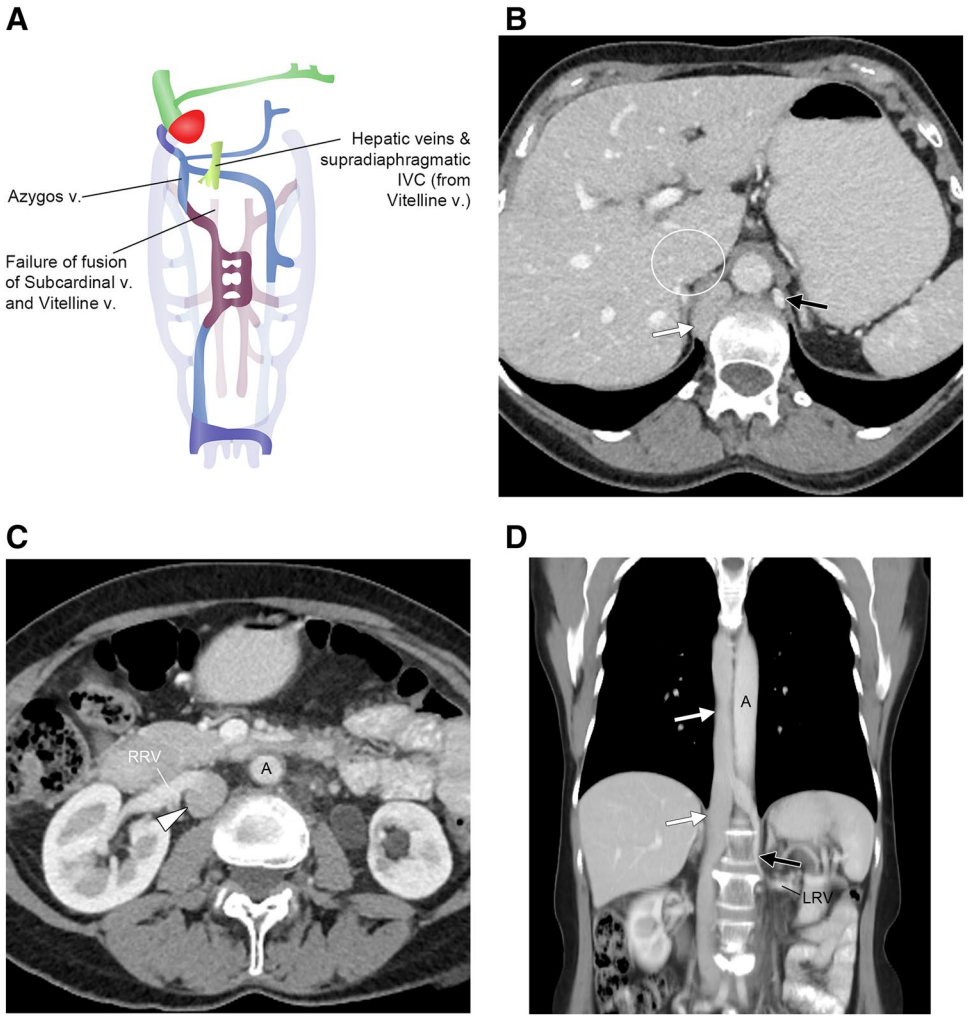

Fig. 5 Azygos continuation of the IVC. **a** Failure of fusion of the subcardinal and vitelline veins results in an interrupted IVC with azygos continuation. *Graphics created by CKS*. **b–d** Contrast-enhanced CT in a 53-year-old woman. **b** Axial CT image at the level of the diaphragmatic crura shows an enlarged azygos vein (white arrow) and a smaller hemiazygos vein (black arrow) and absence of the normal intrahepatic IVC segment (circle). **c** At the level of the right renal vein, the IVC (white arrowhead) receives venous inflow from the right renal vein (RRV). A, aorta. **d** Coronal CT image shows the left renal vein (LRV) draining into the hemiazygos vein (black arrow), which crosses midline in the posterior mediastinum to join the enlarged azygos vein (white arrows), which subsequently drains into the superior vena cava (not shown). In this patient, there was no direct communication between the left renal vein and the IVC. A, aorta

IVC tumor thrombus requires radical surgery but can be performed in those without regional lymph node or distant metastases, with a 5-year survival rate of 68% [11].

Wilms tumor is by far the most common pediatric renal tumor. While intravascular thrombus is common (20–35%), IVC involvement is seen in only 4–10% [12] (Fig. 10). In general, CT is sensitive and specific for pre-operative identification of IVC and right atrial tumor thrombus [13], but ultrasound may be a useful problem-solving adjunct for detecting intravenous extension when CT is equivocal [12].

Adrenal tumors

Adrenocortical carcinoma (ACC) is a rare malignancy of the adrenal gland and may be endocrinologically functional. Age distribution is bimodal, with one peak before 5 years of age and the second in the 4th to 5th decades of life [14]. At diagnosis, ACC tumors tend to be larger than 5 cm, enhance heterogeneously, and have irregular shape with blurred margins [14]. In 9–19% of patients, there is invasion of the tumor into the IVC [14], which is considered Stage III disease [15] (Fig. 11). MRI can be helpful for identifying IVC extension, as well as in differentiating ACC from adenoma or pheochromocytoma [14].

Hepatic tumors

Involvement of the IVC and right atrium by hepatocellular carcinoma (HCC) is not uncommon in advanced disease [16], either due to intracaval extension of hepatic venous tumor thrombus or direct invasion of the IVC wall [17] (Fig. 12). Caval involvement is associated with a poor prognosis in most patients due to increased risk of distant metastases [16]. While direct IVC invasion can be seen with cholangiocarcinoma and metastatic disease, hepatic venous tumor thrombus is uncommon in other primary or secondary hepatic malignancies, and thus is a differentiating feature of HCC [17].

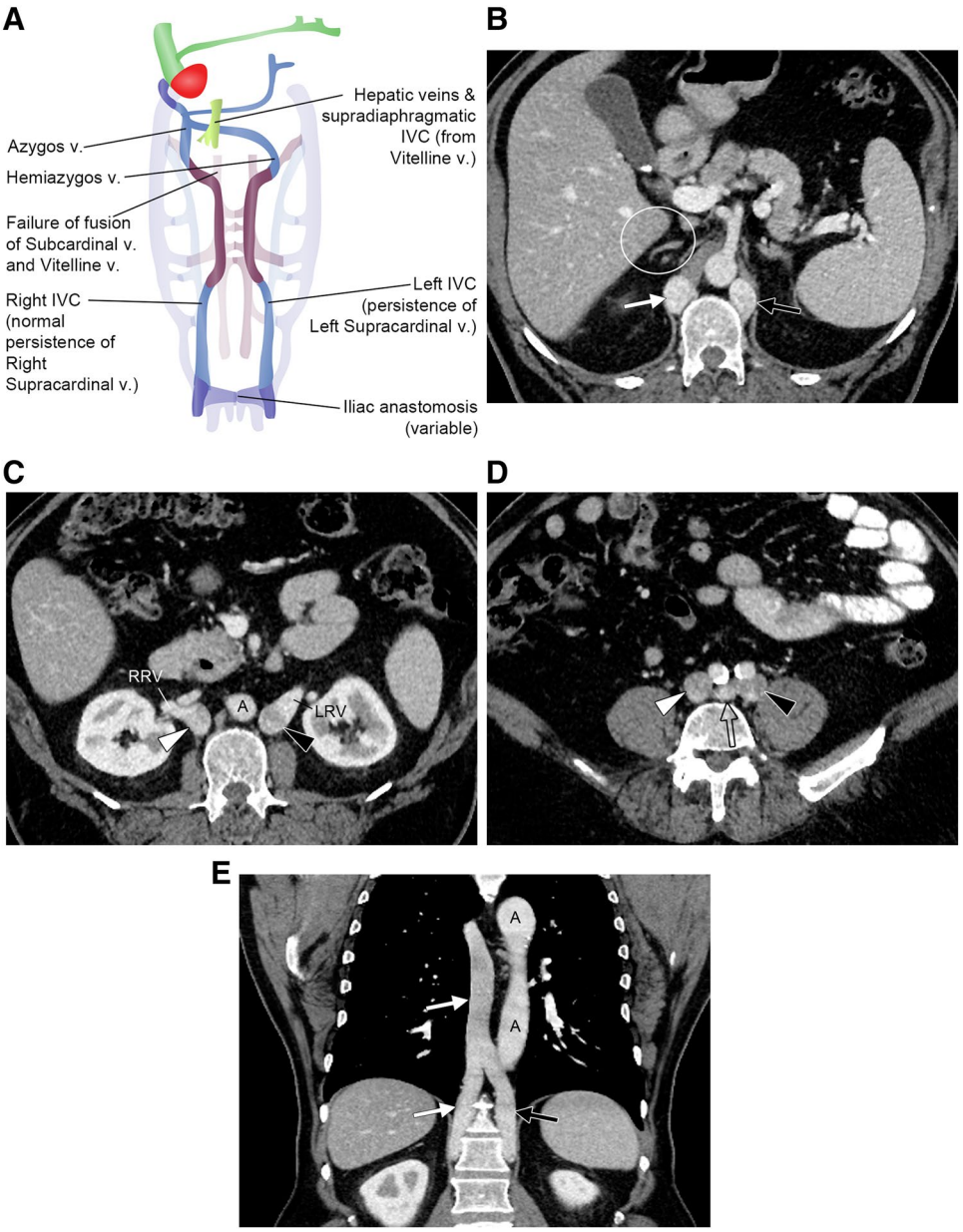

Fig. 6 Azygos and hemiazygos continuation of duplicated IVC. **a** The underlying embryology involves that of duplicated IVC with additional abnormal persistence of the bilateral subcardinal–supracardinal anastomoses without fusion to the vitelline vein. *Graphics created by CKS*. **b**–**e** Contrast-enhanced CT in a 63-year-old man. **b** Axial CT image at the level of the diaphragmatic crura shows an enlarged azygos vein (white arrow) and hemiazygos vein (black arrow) and the absence of the normal intrahepatic IVC segment (circle). **c** The right (white arrowhead) and left (black arrowhead) IVCs receive ipsilateral venous inflow from the right renal vein (RRV) and left renal vein (LRV), respectively. A, aorta. **d** Axial image at the level of the common iliac veins shows persistence of the iliac anastomosis (open arrow) between the right (white arrowhead) and left (black arrowhead) common iliac veins. **e** Coronal CT image of the chest shows the enlarged hemiazygos vein (black arrow) crossing midline and joining the enlarged azygos vein (white arrows), which subsequently drains into the superior vena cava (not shown). A, aorta

Uterine tumors

While benign, leiomyomas of the uterus can demonstrate aggressive features with intravenous growth via the pelvic veins (i.e., intravenous leiomyomatosis) and even extension into the IVC and right atrium [18, 19] (Fig. 13). Unlike primary IVC leiomyosarcoma, leiomyomatosis is continuous with the parent pelvic tumor and not fixed to the IVC wall [18]. Treatment includes not only transcaval excision, but also total abdominal hysterectomy and bilateral salpingo-oophorectomy [18, 19]. Recurrence is likely if excision is incomplete [18].

Primary IVC leiomyosarcoma

Leiomyosarcoma, the primary malignancy arising from the IVC, originates from the smooth muscle cells of the caval wall media and is much less common than secondary tumors (Fig. 14). Given the rarity of the tumor, the true incidence of primary IVC leiomyosarcoma is unclear. The malignancy most commonly affects women in their fifth or sixth decade [20, 21]. The pattern of tumor growth is extraluminal in 59–76%, intraluminal and extraluminal in 16%, and exclusively intraluminal in 20–25% [20, 21]. Central necrosis is common [18].

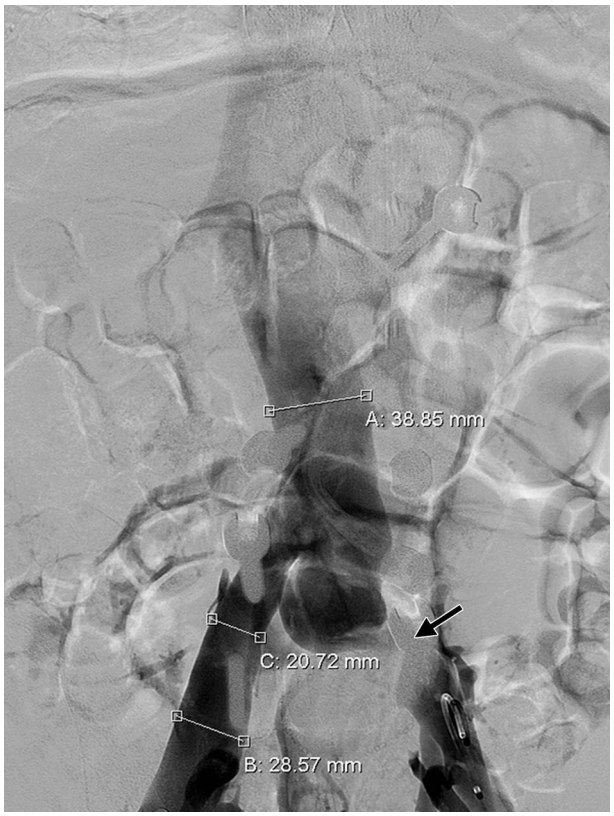

Fig. 7 Megacava. Digital subtraction cavogram in a 65-year-old man shows infrarenal IVC diameter of 3.9 cm, consistent with megacava. For prophylaxis against pulmonary embolism, filters were placed in both common iliac veins (not shown). Incidentally, the left common iliac vein was also stenotic (black arrow), suggesting May–Thurner physiology

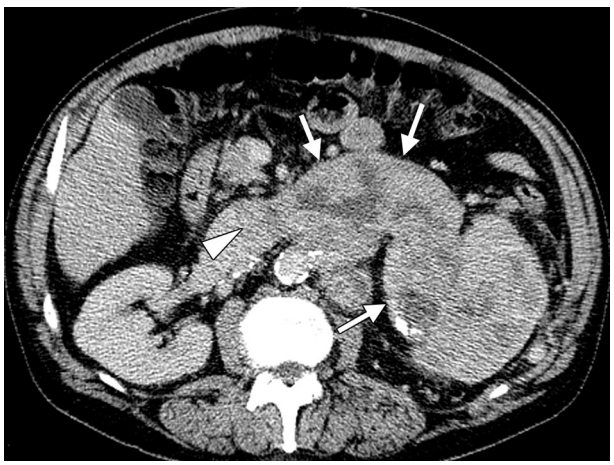

Fig. 8 IVC tumor invasion. Axial contrast-enhanced CT image in a 62-year-old man with RCC shows a large heterogeneously enhancing left renal mass contiguously invading the left renal vein (white arrows) and the IVC (white arrowhead)

IVC leiomyosarcoma distribution is described as segment 1 if infrarenal, segment 2 if suprarenal, and segment 3 if suprahepatic [22] (Fig. 9c). Most tumors involve segment 2, and isolated segment 3 involvement is rare. Involvement of two or more segments occurs in about 21–36% of cases [20, 23]. Treatment is with wide local excision, which may include resection of the aorta or adjacent involved organs such as the kidney, adrenal, and/or liver [20, 24]. Nevertheless, recurrence is highly likely, seen in 94% at 5 years [20].

Non-neoplastic IVC abnormalities

IVC thrombosis

IVC thrombosis is an underdiagnosed phenomenon that is associated with significant morbidity and mortality [25, 26]. Clinical presentation can vary from an asymptomatic incidental imaging finding, to a gradual onset of venous insufficiency symptoms (e.g., lower extremity swelling, lower back, and buttock pain), to an acute severe cardiopulmonary compromise [26].

Etiologies of IVC thrombosis include congenital IVC anomalies and acquired conditions [26]. Although congenital anomalies of the IVC are relatively uncommon and usually accompanied by well-developed collaterals, thrombosis can ensue and become symptomatic if venous hypertension or stasis develops in these collaterals [26]. Acquired IVC thrombosis can occur for a number of reasons. Examples include external compression of the IVC (e.g., adjacent tumor), malignancies involving the IVC wall and lumen, extension of deep vein thrombosis (DVT) from the iliac veins, and damage to the endothelium (e.g., penetrating or iatrogenic injury; presence of a catheter or IVC filter) [26].

Up to 4% of patients with lower extremity DVT may have an associated IVC thrombosis. When left untreated, IVC thrombosis can lead to a myriad of serious clinical problems including post-thrombotic syndrome in up to 90% of patients, severe venous claudication in up to 45% of patients, and pulmonary embolism in up to 30% of patients [25]. Treatment of IVC thrombosis depends on the underlying etiology and acuity. In the case of acute on chronic bland thrombus, catheter-directed thrombolysis and recanalization by balloon angioplasty with or without stenting can be performed to rapidly restore in-line flow.

IVC "pseudothrombus" is an imaging artifact in which heterogeneous opacification of the blood in the IVC can mimic thrombus (Fig. 15). When contrast-enhanced blood flow from a renal vein joins a column of unopacified blood from the infrarenal IVC, it can create the appearance of a filling defect [27]. When delayed images are acquired, the opacification of the blood from different inflow vessels will equilibrate and the filling defect will no longer be visualized, confirming the finding as pseudothrombus.

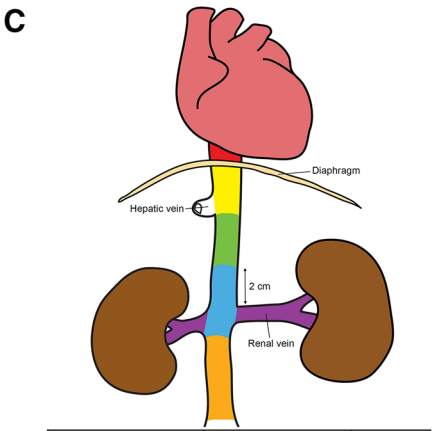

IVC zone	Renal cell carcinoma staging			IVC leiomyosarcoma
	TNM	Robson	Mayo (Neves)	
Supradiaphragmatic IVC	T4b		IV	3
Suprahepatic IVC below diaphragm			III	
Suprarenal IVC > 2cm above RV, below HV	T3c	IIIa	II	2
Suprarenal IVC < 2cm above RV			I	
RV	T3b		0	NA
Below RV	NA	NA	NA	1

HV, hepatic veins. IVC, inferior vena cava. RV, renal veins. NA, not applicable.

◂**Fig. 9** Renal cell carcinoma. **a** Axial contrast-enhanced CT image in a 56-year-old man with renal cell carcinoma shows a large heterogeneously enhancing left renal mass (M) extending into the IVC (black arrowheads). The patient underwent left radical nephrectomy and IVC thrombectomy. **b** Two years later, the patient presented with lower extremity swelling, and coronal T1 contrast-enhanced MR confirmed local disease recurrence (L) with complete IVC occlusion by the tumor (white arrows) and bland iliocaval thrombus (T) inferiorly. **c** Various staging systems for IVC involvement by renal cell carcinoma and IVC leiomyosarcoma and the anatomic segments used to define IVC zones. *Graphics created by CKS*

Fig. 10 Wilms' tumor. **a** Axial and **b** coronal contrast-enhanced CT images in a 4-year-old child with Wilms' tumor. A large heterogeneously enhancing mass (white arrows) arises from the right kidney (K) and invades the IVC (black arrowhead)

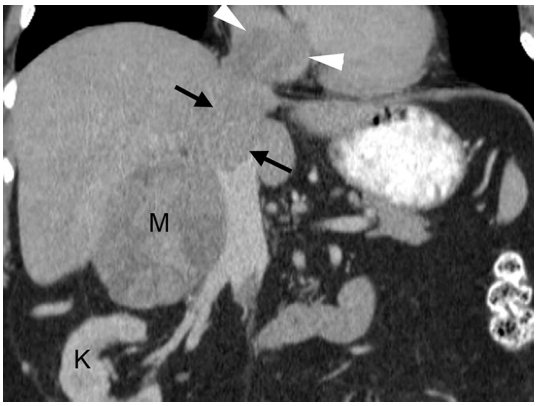

Fig. 11 Adrenocortical carcinoma. Coronal contrast-enhanced CT image in a 60-year-old man with non-functional adrenocortical carcinoma. The heterogeneously enhancing mass (M), which is separate from the right kidney (K), invades the liver and extends into the IVC (black arrows) and right atrium (white arrowheads)

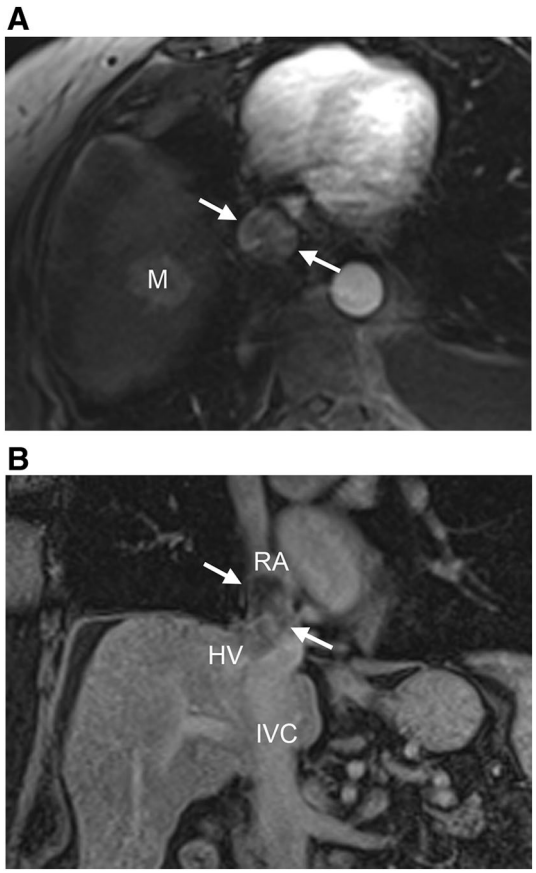

Fig. 12 Hepatocellular carcinoma. **a** Contrast-enhanced MR T1 VIBE axial arterial phase and **b** coronal 4-minute delay phase images demonstrate a primary liver tumor (M) in the hepatic dome of a 79-year-old man. There was direct tumor invasion into the right hepatic vein (HV), suprahepatic IVC (white arrows), and right atrium (RA), with the tumor thrombus demonstrating arterial phase enhancement and delayed washout similar to the primary mass. IVC, inferior vena cava

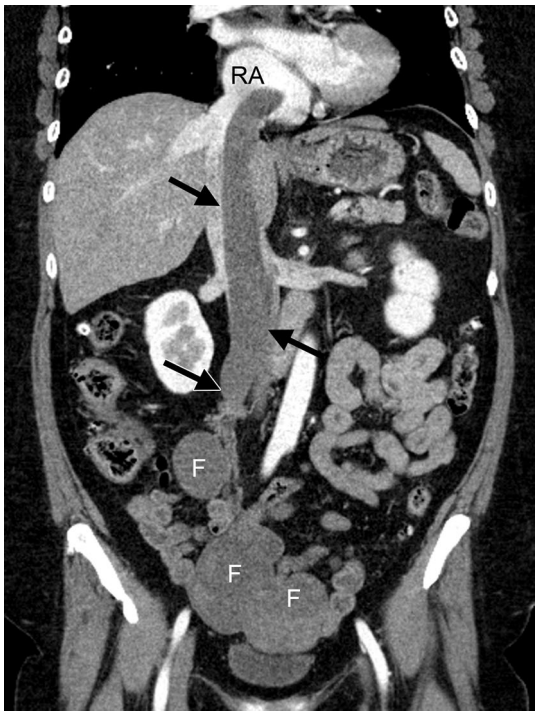

Fig. 13 Intravenous leiomyomatosis. Coronal contrast-enhanced CT in a 54-year-old woman presenting with electrocardiogram changes. A long intracaval tumor (black arrows) contiguously extends from the fibroid uterus (F) to the right gonadal vein, IVC, and right atrium (RA). At surgery, the tumor was not adherent to the vena cava at any point. Pathology revealed benign uterine leiomyoma

Chronic IVC syndrome

Chronic obstruction of the venous outflow through the IVC may result in debilitating symptoms, including abdominal distention and swelling of the lower torso, perineum/genitals, and legs, with associated pain and impaired mobility [28]. Characteristically, the edema associated with the IVC syndrome occurs below the level of the diaphragm. Depending on the location of obstruction, renal insufficiency, hepatomegaly, and ascites may develop. The obstruction may be due to malignancy resulting in extrinsic compression, or less frequently, intrinsic stenosis (Fig. 16). Other causes include iatrogenic complications from a prior surgery (e.g., liver transplant anastomotic stenosis) or endovascular procedure (e.g., chronic IVC filter). Although malignant IVC syndrome was described decades ago with successful endovascular management options suggested since, the disease continues to be undertreated [28–30]. Radiologists may play a key role in early and accurate diagnosis of this condition in appropriate clinical context with careful review of the IVC anatomy.

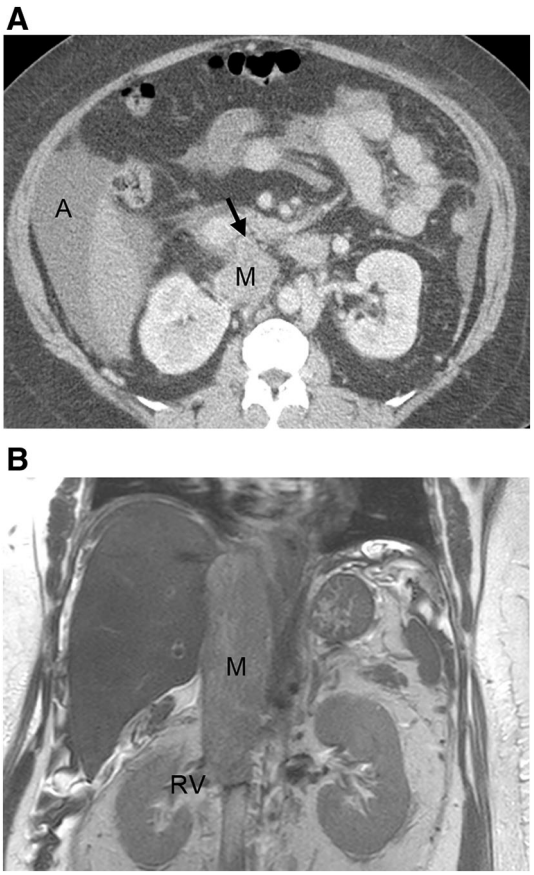

Fig. 14 IVC leiomyosarcoma. **a** Axial contrast-enhanced abdominal CT and **b** coronal T2-weighted SS MR images in a 46-year-old woman presenting with congestive hepatopathy. A mass (M) consistent with IVC leiomyosarcoma distends the IVC from the level of the renal veins (RV) to the diaphragm. Focal anterior caval contour bulge (black arrow) corresponded to the site of tumor origin, as confirmed at surgery. Ascites (A) is present due to portal hypertension related to the obstruction of hepatic venous outflow by the mass

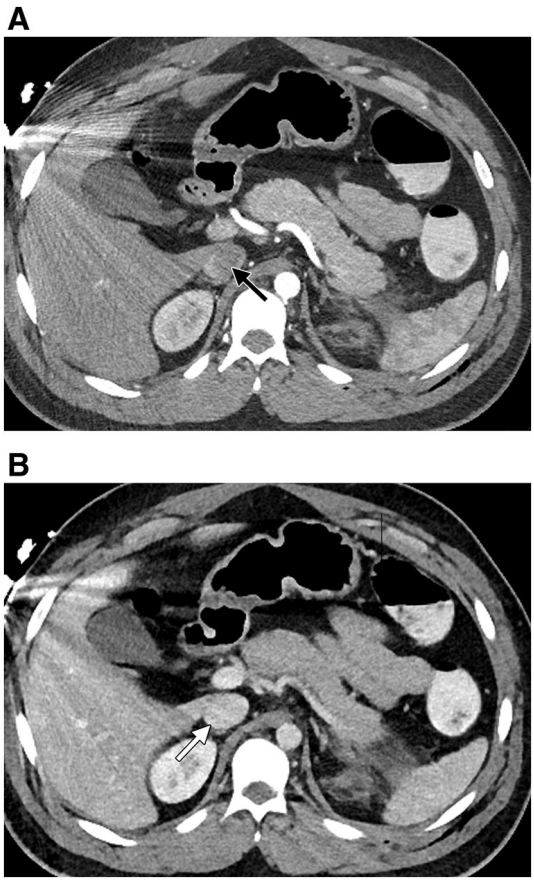

Fig. 15 Pseudothrombosis. Axial images from contrast-enhanced CT in **a** arterial and **b** venous phases. On the arterial phase, inflow of contrast-opacified blood from the renal veins preferentially travels along the periphery of the suprarenal IVC and causes the unopacified blood column from the lower extremities to appear as a filling defect (black arrow). This may be mistaken for IVC thrombus, except that the IVC enhances homogeneously (white arrow) on the venous phase

Aortocaval fistula

Fistula formation between the aorta and IVC can be an acute complication of abdominal aortic aneurysm rupture or repair, or rarely due to trauma. Spontaneous aortocaval fistula may present with abdominal or back pain, pulsating abdominal mass, continuous abdominal bruit, pelvic and lower extremity venous hypertension, shock, or congestive heart failure [31]. This diagnosis is suggested on contrast-enhanced CT when there is early enhancement of the IVC similar to the aorta. Fistulous communication between the aorta and IVC may be directly visualized (Fig. 17). Treatment can be surgical or endovascular.

Trauma

IVC injury is a rare event for both blunt and penetrating traumas and has a high mortality rate [32, 33]. While some patients with IVC trauma are too unstable for imaging, CT signs of IVC injury include retroperitoneal hematoma with or without IVC contour abnormality and active contrast extravasation [34] (Fig. 18a). Hepatic laceration may coexist, and injuries of the retrohepatic IVC carry a poor prognosis [33, 34]. Given the low intraluminal pressure, self-tamponade can occur in the absence of significant concomitant disruption of the surrounding soft tissues.

When not directly involved in trauma, flattening of the IVC has been reported as an indicator of hypovolemia [35] and, to variable degrees, a predictor of present or subsequent development of shock, need for aggressive resuscitation and transfusion, intensive care unit admission, increased length of hospital stay, and higher mortality [36–42] (Fig. 18b). IVC

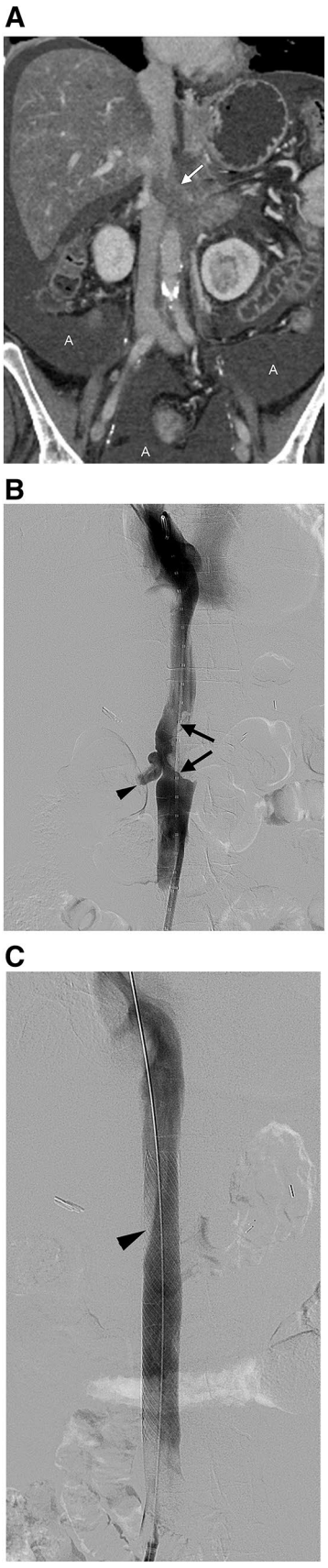

Fig. 16 Malignant IVC syndrome managed with stenting. **a** Coronal ▶ contrast-enhanced CT image in a 67-year-old woman with metastatic pancreatic cancer presenting with lower body swelling and abdominal distention demonstrates left renal vein tumor thrombus (white arrow) and large volume ascites (A). **b** Digital subtraction cavogram demonstrates bulky renal vein tumor thrombus resulting in renal segment and suprarenal IVC stenosis (black arrows). Reflux into the right renal vein (black arrowhead) is noted. Pressure gradient across the lesion was estimated at 12 mmHg. **c** Digital subtraction cavogram following placement of a 22-mm Wallstent (Boston Scientific, Marlborough, MA) demonstrates resolution of the IVC stenosis and normal inflow from the right renal vein (black arrowhead). The pressure gradient was reduced to 1 mm. The patient's symptoms quickly improved with resolution of her lower extremity edema within 48 h

diameter can be measured on ultrasound, although most published data are derived from CT. It should be noted, however, that there is neither a universally accepted standard for measuring the IVC caliber nor a diagnostic threshold for clinically meaningful narrowing. Anteroposterior IVC diameter has been used, with reported threshold values ranging from 9 to 13 mm [36, 37]. Alternatively, a ratio of transverse to anteroposterior diameters has been advocated, with cutoff values ranging from 1.9 to 3 [38–42].

Flattened IVC constitutes one of the CT signs of clinically significant hypoperfusion in adult blunt trauma patients (i.e., hypoperfusion complex) along with flattened renal veins, active contrast extravasation, free peritoneal fluid, and small bowel enhancement and dilation [43]. Collapsed IVC may also be a helpful predictor of clinical outcome in pediatric and elderly trauma patients, in whom heart rate and blood pressure may be less reliable indicators of hypovolemia [44, 45].

IVC interventions

IVC filter

Understanding variant IVC anatomy helps avoid problems in several situations during IVC filter placement. A duplicated IVC is especially important to recognize. In this situation, placement of an IVC filter only in the right IVC results in incomplete protection given the remaining route for venous thromboembolism along the left IVC. Two IVC filters are necessary to avoid pulmonary embolism (Fig. 2e). Similarly, clearly delineating renal vein anatomy is important in IVC filter placement, as infrarenal placement is desired to prevent renal venous thrombosis.

In cases of megacava (Fig. 7), the only approved IVC filter is the Bird's Nest filter (Cook, Bloomington, IN). Alternatively, two optionally retrievable filters can be placed within the bilateral common iliac veins.

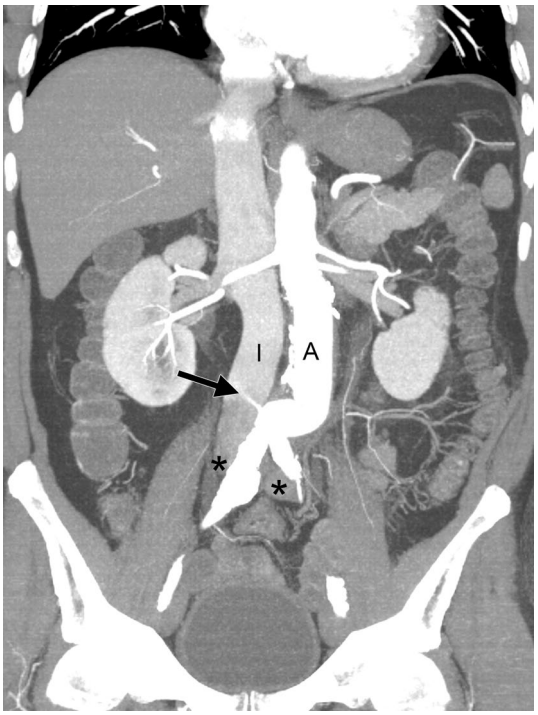

Fig. 17 Aortocaval fistula. Coronal maximum-intensity projection image from CT angiography in a 64-year-old man status post repair of abdominal aortic aneurysm 3 years prior, now presenting with lower extremity claudication and dyspnea on exertion. A jet of contrast (black arrow) is seen extending into the IVC from the densely opacified aortic lumen (A), resulting in early opacification of the IVC (I) compared to the iliac veins (*)

IVC stent placement

Palliative IVC stent placement has been shown to improve symptoms in multiple retrospective series [30, 46, 47] (Fig. 16). One prospective study of 7 patients with malignant IVC obstruction showed improvements in physiologic and biochemical parameters after IVC stenting, including decreased edema, ascites, and azotemia in the days following stenting [48]. A larger retrospective study of 57 patients showed a decrease in leg edema following IVC stenting in 83% and 86% of patients at 7 and 30 days, respectively [30].

The feared complication of stent migration occurs infrequently, with rare reported cases of intracardiac embolization [30, 49, 50]. An acute increase in venous return to the heart after stent placement may result in hemodynamic changes [51]. Although cardiac complications are rare, IVC stenting should proceed with caution in patients with known cardiac dysfunction [51]. Preprocedural echocardiogram should be considered to assess the baseline cardiac function when evaluating patients for the procedure.

Fig. 18 Trauma. **a** Axial contrast-enhanced CT image in a 23-year-old man with a transabdominal gunshot wound shows retroperitoneal hematoma surrounding a focal outpouching of the IVC (white arrow). Also visible are hemoperitoneum with active hemorrhage at the liver capsule (black arrowhead), free air medial to the liver, and duodenal injury. **b** Axial contrast-enhanced CT image in a 75-year-old woman hypotensive after being hit by a car shows flattening of the IVC (white arrow) at the level of the renal veins, as well as diffuse bowel wall thickening and hyperenhancement representing shock bowel

IVC tumor biopsy

Although malignant extension of an abdominal tumor into the IVC can readily suggest diagnosis based on the organ of origin, a tumor involving only the IVC can pose more of a diagnostic challenge. Endovascular biopsy can be a valuable technique when the pathologic diagnosis of the tumor is desired [18] (Fig. 19). Access into the IVC lumen is easily and safely achieved via an internal jugular vein or common femoral vein. Venography precedes biopsy to better delineate the tumor and allow for planning of a safe biopsy pass. Intravascular ultrasound can be employed as an adjunct technique to guide and document needle passage in real time.

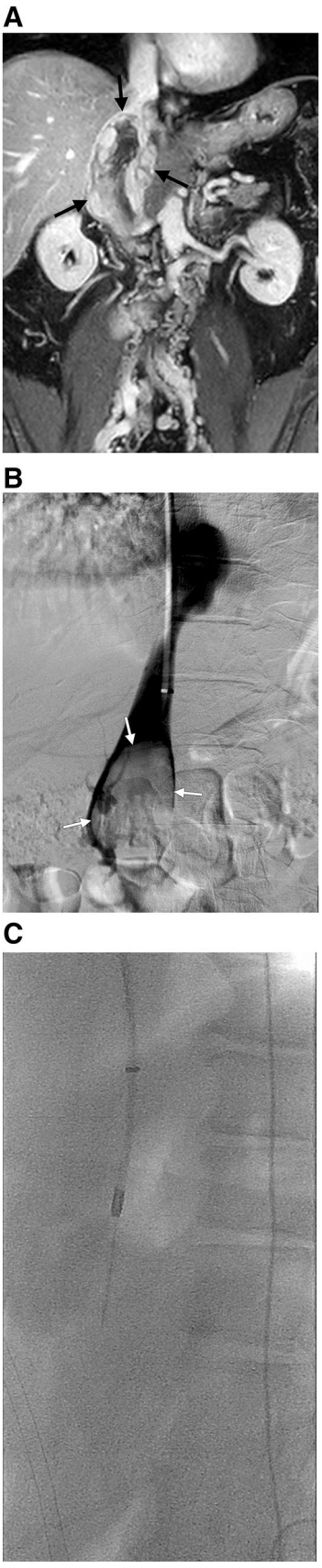

Fig. 19 Endovascular biopsy. A 45-year-old man presented with lower extremity swelling. **a** Coronal image from contrast-enhanced MR demonstrated a heterogeneously enhancing mass (black arrows) within the juxtarenal inferior vena cava. **b** Digital subtraction venography outlined the superior aspects of the expansile mass (white arrows). **c** Following the introduction of a straightened transjugular liver biopsy set (Argon Dextera TLAB Patel Set; US Biopsy; Franklin, IN), multiple biopsy cores were obtained, which confirmed leiomyosarcoma

Tunneled translumbar central venous catheter placement

In a small subgroup of patients presenting with difficult vascular access (e.g., parenteral nutrition- or dialysis-dependent patients), all potential sites for central venous access, including internal jugular, subclavian, and femoral veins, may be exhausted. In this uncommon clinical scenario, consideration can be given to direct translumbar IVC access [52, 53] (Fig. 20). Prior to translumbar IVC catheter placement, imaging should be reviewed to confirm patency of the IVC. Using image guidance (ultrasound, CT, or C-arm CT), the IVC can be entered with the patient in a prone or left lateral decubitus position [52, 53]. Catheters are tunneled from the right flank for comfort and ease of access.

Conclusion

The IVC can often be overlooked in abdominal imaging. However, it is an important structure that may be involved in various pathologic processes with potentially devastating acute and chronic symptoms. A comprehensive understanding of IVC anatomy, variants, and diseases is essential for diagnosis and treatment recommendations by the radiologist.

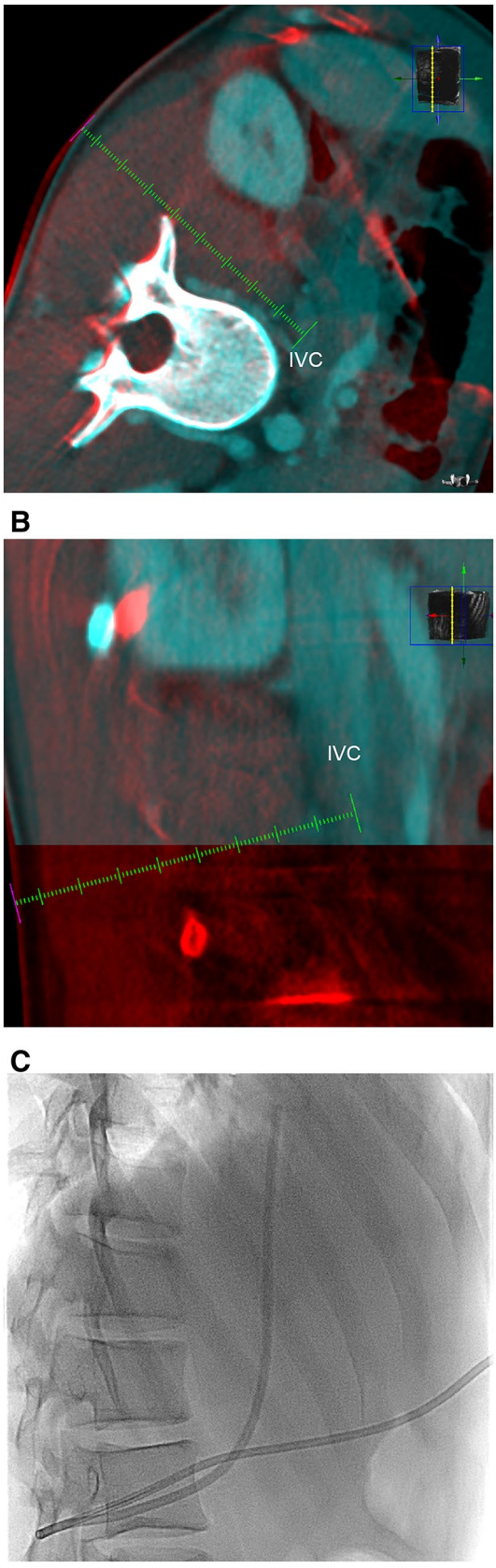

◂ **Fig. 20** Tunneled translumbar central venous catheter. A 16-year-old boy presented with anterior mediastinal lymphoma and SVC obstruction. A tunneled central venous catheter for the initiation of chemotherapy was requested with avoidance of femoral access due to increased central line infection concerns. **a** Planning axial and **b** progress sagittal views from a 3-dimensional navigational overlay (XperGuide, Philips, Eindhoven, the Netherlands) based on an intraprocedural cone beam CT fused with prior contrast-enhanced CT were used to guide translumbar caval access and **c** subsequent tunneled central venous catheter placement. IVC, Inferior Vena Cava

Compliance with ethical standards

Conflict of interest The authors declare that there is no conflict of interest regarding the publication of this article.

References

1. Bass JE, Redwine MD, Kramer LA, Huynh PT, Harris JH, Jr. Spectrum of congenital anomalies of the inferior vena cava: cross-sectional imaging findings. Radiographics 2000;20:639-52.
2. Ginaldi S, Chuang VP, Wallace S. Absence of hepatic segment of the inferior vena cava with azygous continuation. Journal of computer assisted tomography 1980;4:112-4.
3. Haswell DM, Berrigan TJ, Jr. Anomalous inferior vena cava with accessory hemiazygos continuation. Radiology 1976;119:51-4.
4. Ettinger E, Steinberg I. Angiocardiographic measurement of the cardiac segment of the inferior vena cava in health and in cardiovascular disease. Circulation 1962;26:508-15.
5. Prince MR, Novelline RA, Athanasoulis CA, Simon M. The diameter of the inferior vena cava and its implications for the use of vena caval filters. Radiology 1983;149:687-9.
6. Smillie RP, Shetty M, Boyer AC, Madrazo B, Jafri SZ. Imaging evaluation of the inferior vena cava. Radiographics 2015;35:578-92.
7. Kraft C, Schuettfort G, Weil Y, et al. Thrombosis of the inferior vena cava and malignant disease. Thrombosis research 2014;134:668-73.
8. Hollenbeck ST, Grobmyer SR, Kent KC, Brennan MF. Surgical treatment and outcomes of patients with primary inferior vena cava leiomyosarcoma. Journal of the American College of Surgeons 2003;197:575-9.
9. Sheth S, Scatarige JC, Horton KM, Corl FM, Fishman EK. Current concepts in the diagnosis and management of renal cell carcinoma: role of multidetector ct and three-dimensional CT. Radiographics 2001;21 Spec No:S237-54.
10. Psutka SP, Boorjian SA, Thompson RH, et al. Clinical and radiographic predictors of the need for inferior vena cava resection during nephrectomy for patients with renal cell carcinoma and caval tumour thrombus. BJU international 2015;116:388-96.
11. Neves RJ, Zincke H. Surgical treatment of renal cancer with vena cava extension. British journal of urology 1987;59:390-5.
12. Al Diab A, Hirmas N, Almousa A, et al. Inferior vena cava involvement in children with Wilms tumor. Pediatric surgery international 2017;33:569-73.
13. Khanna G, Rosen N, Anderson JR, et al. Evaluation of diagnostic performance of CT for detection of tumor thrombus in children with Wilms tumor: a report from the Children's Oncology Group. Pediatric blood & cancer 2012;58:551-5.

14. Ng L, Libertino JM. Adrenocortical carcinoma: diagnosis, evaluation and treatment. The Journal of urology 2003;169:5-11.
15. Libe R, Borget I, Ronchi CL, et al. Prognostic factors in stage III-IV adrenocortical carcinomas (ACC): an European Network for the Study of Adrenal Tumor (ENSAT) study. Annals of oncology : official journal of the European Society for Medical Oncology 2015;26:2119-25.
16. Chang JY, Ka WS, Chao TY, Liu TW, Chuang TR, Chen LT. Hepatocellular carcinoma with intra-atrial tumor thrombi. A report of three cases responsive to thalidomide treatment and literature review. Oncology 2004;67:320-6.
17. Kaneko T, Nakao A, Nomoto S, Endo T, Itoh S, Takagi H. Intracaval endovascular ultrasonography for preoperative assessment of retrohepatic inferior vena cava infiltration by malignant hepatic tumors. Hepatology (Baltimore, Md) 1996;24:1121-7.
18. Armstrong PJ, Franklin DP. Pararenal vena cava leiomyosarcoma versus leiomyomatosis: difficult diagnosis. Journal of vascular surgery 2002;36:1256-9.
19. Peng HJ, Zhao B, Yao QW, Qi HT, Xu ZD, Liu C. Intravenous leiomyomatosis: CT findings. Abdominal imaging 2012;37:628-31.
20. Wachtel H, Gupta M, Bartlett EK, et al. Outcomes after resection of leiomyosarcomas of the inferior vena cava: a pooled data analysis of 377 cases. Surgical oncology 2015;24:21-7.
21. Mingoli A, Cavallaro A, Sapienza P, Di Marzo L, Feldhaus RJ, Cavallari N. International registry of inferior vena cava leiomyosarcoma: analysis of a world series on 218 patients. Anticancer research 1996;16:3201-5.
22. Kulaylat MN, Karakousis CP, Doerr RJ, Karamanoukian HL, O'Brien J, Peer R. Leiomyosarcoma of the inferior vena cava: a clinicopathologic review and report of three cases. Journal of surgical oncology 1997;65:205-17.
23. Kieffer E, Alaoui M, Piette JC, Cacoub P, Chiche L. Leiomyosarcoma of the inferior vena cava: experience in 22 cases. Annals of surgery 2006;244:289-95.
24. Sulpice L, Rayar M, Levi Sandri GB, et al. Leiomyosarcoma of the inferior vena cava. Journal of visceral surgery 2016;153:161-5.
25. Alkhouli M, Morad M, Narins CR, Raza F, Bashir R. Inferior Vena Cava Thrombosis. JACC Cardiovascular interventions 2016;9:629-43.
26. McAree BJ, O'Donnell ME, Fitzmaurice GJ, Reid JA, Spence RA, Lee B. Inferior vena cava thrombosis: a review of current practice. Vascular medicine (London, England) 2013;18:32-43.
27. Vogelzang RL, Gore RM, Neiman HL, Smith SJ, Deschler TW, Vrla RF. Inferior vena cava CT pseudothrombus produced by rapid arm-vein contrast infusion. AJR American journal of roentgenology 1985;144:843-6.
28. Hartley JW, Awrich AE, Wong J, Stevens K, Fletcher WS. Diagnosis and treatment of the inferior vena cava syndrome in advanced malignant disease. American journal of surgery 1986;152:70-4.
29. Oudkerk M, Heystraten FM, Stoter G. Stenting in malignant vena caval obstruction. Cancer 1993;71:142-6.
30. Devcic Z, Techasith T, Banerjee A, Rosenberg JK, Sze DY. Technical and Anatomic Factors Influencing the Success of Inferior Vena Caval Stent Placement for Malignant Obstruction. Journal of vascular and interventional radiology : JVIR 2016;27:1350-60. e1.
31. Davidovic L, Dragas M, Cvetkovic S, Kostic D, Cinara I, Banzic I. Twenty years of experience in the treatment of spontaneous aorto-venous fistulas in a developing country. World journal of surgery 2011;35:1829-34.
32. van Rooyen PL, Karusseit VO, Mokoena T. Inferior vena cava injuries: a case series and review of the South African experience. Injury 2015;46:71-5.
33. Buckman RF, Pathak AS, Badellino MM, Bradley KM. Injuries of the inferior vena cava. The Surgical clinics of North America 2001;81:1431-47.
34. Tsai R, Raptis C, Schuerer DJ, Mellnick VM. CT Appearance of Traumatic Inferior Vena Cava Injury. AJR American journal of roentgenology 2016;207:705-11.
35. Dipti A, Soucy Z, Surana A, Chandra S. Role of inferior vena cava diameter in assessment of volume status: a meta-analysis. The American journal of emergency medicine 2012;30:1414-9.e1.
36. Anand T, vanSonnenberg E, Gadani K, Skinner R. A snapshot of circulation failure following acute traumatic injury: The expansion of computed tomography beyond injury diagnosis. Injury 2016;47:50-2.
37. Takada H, Hifumi T, Yoshioka H, et al. Initial inferior vena cava diameter predicts massive transfusion requirements in blunt trauma patients: A retrospective cohort study. The American journal of emergency medicine 2018;36:1155-9.
38. Johnson JJ, Garwe T, Albrecht RM, et al. Initial inferior vena cava diameter on computed tomographic scan independently predicts mortality in severely injured trauma patients. The journal of trauma and acute care surgery 2013;74:741-5; discussion 5-6.
39. Li Y, Zhang LY, Wang Y, Zhang WG. The flatness index of inferior vena cava is useful in predicting hypovolemic shock in severe multiple-injury patients. The Journal of emergency medicine 2013;45:872-8.
40. Liao YY, Lin HJ, Lu YH, Foo NP, Guo HR, Chen KT. Does CT evidence of a flat inferior vena cava indicate hypovolemia in blunt trauma patients with solid organ injuries? The Journal of trauma 2011;70:1358-61.
41. Matsumoto S, Sekine K, Yamazaki M, et al. Predictive value of a flat inferior vena cava on initial computed tomography for hemodynamic deterioration in patients with blunt torso trauma. The Journal of trauma 2010;69:1398-402.
42. Nguyen A, Plurad DS, Bricker S, et al. Flat or fat? Inferior vena cava ratio is a marker for occult shock in trauma patients. The Journal of surgical research 2014;192:263-7.
43. Smithson L, Morrell J, Kowalik U, Flynn W, Guo WA. Correlation of computed tomographic signs of hypoperfusion and clinical hypoperfusion in adult blunt trauma patients. The journal of trauma and acute care surgery 2015;78:1162-7.
44. Barber JL, Touska P, Negus AS. Inferior vena cava calibre on paediatric trauma CT may be a useful predictor for the development of shock. Clinical radiology 2016;71:565-9.
45. Milia DJ, Dua A, Paul JS, Tolat P, Brasel KJ. Clinical utility of flat inferior vena cava by axial tomography in severely injured elderly patients. The journal of trauma and acute care surgery 2013;75:1002-5; discussion 5.
46. Entwisle KG, Watkinson AF, Hibbert J, Adam A. The use of the Wallstent endovascular prosthesis in the treatment of malignant inferior vena cava obstruction. Clinical radiology 1995;50:310-3.
47. Brountzos EN, Binkert CA, Panagiotou IE, Petersen BD, Timmermans H, Lakin PC. Clinical outcome after intrahepatic venous stent placement for malignant inferior vena cava syndrome. Cardiovascular and interventional radiology 2004;27:129-36.
48. Kishi K, Sonomura T, Fujimoto H, et al. Physiologic effect of stent therapy for inferior vena cava obstruction due to malignant liver tumor. Cardiovascular and interventional radiology 2006;29:75-83.
49. Hesterberg K, Babu A, Frank M, Hogan S, Krantz MJ. Severe tricuspid regurgitation due to valvular entrapment of an inferior vena cava stent. Clinical case reports 2017;5:130-3.
50. Toyoda N, Torregrossa G, Itagaki S, Pawale A, Reddy R. Intracardiac migration of vena caval stent: decision-making and treatment considerations. Journal of cardiac surgery 2014;29:320-2.
51. Yamagami T, Nakamura T, Kato T, Iida S, Nishimura T. Hemodynamic changes after self-expandable metallic stent therapy for

vena cava syndrome. AJR American journal of roentgenology 2002;178:635-9.
52. Herscu G, Woo K, Weaver FA, Rowe VL. Use of unconventional dialysis access in patients with no viable alternative. Annals of vascular surgery 2013;27:332-6.
53. Gupta A, Karak PK, Saddekni S. Translumbar inferior vena cava catheter for long-term hemodialysis. Journal of the American Society of Nephrology : JASN 1995;5:2094-7.

Publisher's Note Springer Nature remains neutral with regard to jurisdictional claims in published maps and institutional affiliations.